Viscosity Increase with Temperature in Cationic Surfactant Solutions Due to the Growth of Wormlike Micelles

Gokul C. Kalur,† Bradley D. Frounfelker, Bani H. Cipriano, Alexander I. Norman, and Srinivasa R. Raghavan*

Department of Chemical Engineering, University of Maryland, College Park, Maryland 20742-2111

Received July 28, 2005. In Final Form: September 14, 2005

Wormlike micellar solutions based on ionic surfactants typically show an exponential decrease in viscosity upon heating. Here, we report the unusual observation of an *increasing* viscosity with temperature in certain cationic wormlike micellar solutions. The solutions contain a cationic surfactant with an erucyl (C_{22}, mono-unsaturated) tail and an organic salt, sodium hydroxynaphthalene carboxylate (SHNC). When these solutions are heated, their zero-shear viscosity increases over a range of temperatures. In some cases, the viscosity reaches a peak at a certain temperature and then decreases with further heating. The magnitude of the viscosity increase, the onset of this increase, and the peak temperature can all be tuned by varying the SHNC concentration. Small-angle neutron scattering is used to study the origin of this unusual rheological behavior. The data reveal that the contour length of the micelles increases with temperature, in tandem with the rise in viscosity. A possible explanation for the contour length increase, based on a temperature-dependent counterion binding, is discussed.

1. Introduction

Over the past several years, there has been a great deal of interest in the aqueous self-assembly of cationic surfactants into threadlike or wormlike micelles.[1,2] These micelles are long, flexible, cylindrical chains with contour lengths on the order of a few micrometers. The entanglement of these wormlike chains into a transient network imparts viscoelastic properties to the solution. Wormlike micelles are much like polymers with the important exception that the micelles are in thermal equilibrium with their monomers.[3] The average micellar length $\bar{L}$ is thus a thermodynamic quantity, and it responds to changes in solution composition and temperature.

Typically, when a wormlike micellar solution is heated, the micellar contour length $\bar{L}$ decays exponentially with temperature.[3,4] The reason for this is that, at higher temperatures, surfactant unimers can hop more rapidly between the cylindrical body and the hemispherical end-cap of the worm (the end-cap is energetically unfavorable over the body by a factor equal to the end-cap energy E_c). Thus, because the end-cap constraint is less severe at higher temperatures, the worms grow to a lesser extent. The reduction in micellar length, in turn, leads to an exponential decrease in rheological properties such as the zero-shear viscosity η_0 and the relaxation time t_R.[4−6] Accordingly, an Arrhenius plot of ln η_0 versus $1/T$ (where T is the absolute temperature) falls on a straight line, the slope of which yields the flow activation energy E_a. Values of E_a ranging from 70 to 300 kJ/mol have been reported for various micellar solutions.[4−6]

In this paper, we report an unexpected *opposite* trend in rheological behavior for certain wormlike micellar solutions as a function of temperature. Instead of dropping exponentially, the zero-shear viscosity η_0 *increases* over a range of temperatures. We use small-angle neutron scattering (SANS) to show that the increase in viscosity is associated with an increase in micellar length. The system in which we see this unusual behavior is a mixture of a C_{22}−tailed cationic surfactant, erucyl *bis*-(hydroxyethyl)methylammonium chloride (EHAC) and an aromatic salt, sodium hydroxynaphthalene carboxylate (SHNC) (Scheme 1). The counterion in SHNC is hydrophobic due to its naphthalene ring and thus has a tendency to bind strongly with cationic micelles.[7,8] The binding of SHNC reduces the surface charge on EHAC micelles and thereby promotes the growth of long worms. While a few mM of SHNC are sufficient to induce micellar growth, the increase in viscosity with temperature is seen only at much higher SHNC concentrations.

Previously, one of us had studied the same cationic surfactant, EHAC, with a different aromatic salt, sodium salicylate (NaSal).[4,9] The crucial difference between NaSal and SHNC is the presence of an extra benzene ring in SHNC (see Scheme 1). Thus, it is useful to compare the present EHAC−SHNC system with the previous EHAC−NaSal system. Both systems exhibit an unusual feature in their phase behavior, viz. the presence of cloud points (liquid−liquid phase separation upon heating) at intermediate salt concentrations.[9] We will begin this paper by reporting the phase behavior of EHAC−SHNC as a function of salt and temperature and thereafter proceed

* To whom correspondence should be addressed. E-mail: sraghava@eng.umd.edu.

† Present address: Irix Pharmaceuticals, Inc., Florence, SC.

(1) Hoffmann, H. Viscoelastic Surfactant Solutions. In *Structure and Flow in Surfactant Solutions*; Herb, C. A., Prud'homme, R. K., Eds.; American Chemical Society: Washington, DC, 1994; p 2.

(2) Yang, J. *Curr. Opin. Colloid Interface Sci.* **2002**, *7*, 276.

(3) Cates, M. E.; Candau, S. J. *J. Phys.-Condens. Matter* **1990**, *2*, 6869.

(4) Raghavan, S. R.; Kaler, E. W. *Langmuir* **2001**, *17*, 300.

(5) Makhloufi, R.; Cressely, R. *Colloid Polym. Sci.* **1992**, *270*, 1035.

(6) Ponton, A.; Schott, C.; Quemada, D. *Colloids Surf., A* **1998**, *145*, 37.

(7) Mishra, B. K.; Samant, S. D.; Pradhan, P.; Mishra, S. B.; Manohar, C. *Langmuir* **1993**, *9*, 894.

(8) Horbaschek, K.; Hoffmann, H.; Thunig, C. *J. Colloid Interface Sci.* **1998**, *206*, 439.

(9) Raghavan, S. R.; Edlund, H.; Kaler, E. W. *Langmuir* **2002**, *18*, 1056.

10.1021/la052069w CCC: $30.25
Published on Web 10/29/2005

Scheme 1. Chemical Structures of the Surfactant and Salts Used

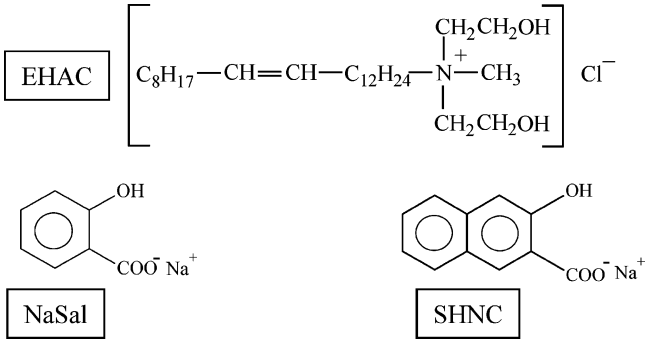

to discuss the unusual viscosity results that are observed in one region of the phase diagram.

2. Experimental Section

Materials. The EHAC surfactant was a commercial product from Akzo Nobel, Chicago, IL, and its chemical structure is shown below. Details on this material have been reported in our previous studies.[4,9] The same material has also been investigated by other groups.[10−14]

SHNC (99% purity) was purchased from Aldrich. Solutions containing surfactant and salt were prepared using distilled, deionized water.

Phase Behavior. Phase behavior was recorded by visual observation. The phase boundaries as a function of temperature were determined by noting the incipient formation of a second phase on heating or cooling (transitions were always determined from one-phase to two-phase states). At the cloud point, the entire sample turned cloudy on heating. The transition temperatures reported here are reproducible to ±0.5 °C.

Rheology. Steady and dynamic rheological experiments were performed on a Rheometrics SR5 stress-controlled rheometer. A couette cell was used with a cup of 27.5 mm diameter and a bob 25 mm × 37.5 mm. The cell was heated by fluid circulating from a Julabo high-temperature bath, and the temperature was controlled to ±0.1 °C. Samples were equilibrated at the temperature of interest for at least 20 min prior to experimentation. A solvent trap was used to minimize water evaporation. Frequency spectra were conducted in the linear viscoelastic regime of the samples, as determined from dynamic strain sweep measurements.

Small-Angle Neutron Scattering (SANS). SANS measurements were made on the NG-3 (30 m) beamline at the NIST Center for Neutron Research (NCNR) in Gaithersburg, MD. Samples were studied in 2 mm quartz cells. The scattering spectra were corrected and placed on an absolute scale using calibration standards provided by NIST. The data are shown for the radially averaged, absolute intensity I versus the scattering vector $q = 4\pi \sin(\theta/2)/\lambda$, where λ is the wavelength of incident neutrons and θ is the scattering angle.

3. Results

Phase Behavior. We begin by describing the phase behavior of EHAC/SHNC solutions at a fixed EHAC concentration (c_{EHAC}) of 40 mM. Figure 1 is a plot of temperature vs salt concentration, and we compare the results for SHNC (Figure 1b) with those previously reported[9] for NaSal (Figure 1a). As mentioned earlier,

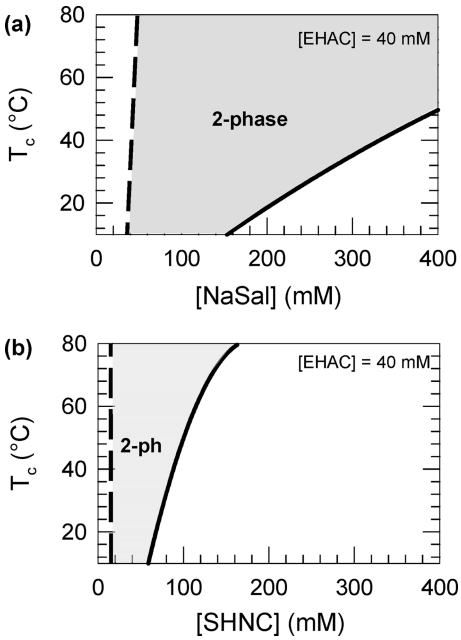

Figure 1. Phase behavior of 40 mM EHAC solutions as a function of temperature and salt concentration. Data are shown for two salts: (a) NaSal (replotted from ref 9) and (b) SHNC. The cloud-point curve in each case is drawn as a solid curve.

this comparison is interesting because the SHNC molecule is identical to NaSal except for the presence of a second benzene ring. From Figure 1, we conclude that the SHNC phase diagram shows *all the same features* as the NaSal one, the difference being that each phase boundary is shifted to a lower salt concentration (along the x axis). In other words, the SHNC phase diagram is a compressed version of the NaSal one, while qualitatively remaining the same.

The progression in EHAC/SHNC phase behavior, proceeding from low to high salt concentration (c_{SHNC}), is as follows. In the low-salt limit, the samples are one-phase and highly viscous. In fact, adding less than 10 mM of SHNC to 40 mM EHAC is enough to induce significant micellar growth. When c_{SHNC} exceeds about 15 mM, however, the samples phase-separate into two co-existing liquid phases. Similar results are observed for NaSal, with a micellar region at low salt, followed by phase-separation around 32 mM salt.[9] For both SHNC and NaSal, the biphasic samples are converted into single-phase micellar solutions by the addition of higher concentrations of salt. At 25 °C, the micellar phase is recovered around 80 mM SHNC; for comparison, the corresponding value for NaSal is around 220 mM.

Remarkably, in the high-salt region of both EHAC/SHNC and EHAC/NaSal phase diagrams, we observe the appearance of *cloud-point behavior*.[9] That is, these high-salt samples phase-separate into co-existing liquid phases when *heated* beyond their corresponding cloud-point curves (shown by solid lines in Figure 1). Cloud-point phenomena in ionic surfactant solutions are highly unusual,[9,15,16] and their origins in EHAC/salt mixtures are still a matter of speculation. Note that the cloud-point phenomenon is seen over a wider range of salt concentrations for NaSal compared to SHNC (reiterating our earlier point that the SHNC phase diagram is a compressed version of the NaSal one). In the case of SHNC, cloud

(10) Croce, V.; Cosgrove, T.; Maitland, G.; Hughes, T.; Karlsson, G. *Langmuir* **2003**, *19*, 8536.
(11) Couillet, I.; Hughes, T.; Maitland, G.; Candau, F.; Candau, S. J. *Langmuir* **2004**, *20*, 9541.
(12) Siriwatwechakul, W.; Lafleur, T.; Prud'homme, R. K.; Sullivan, P. *Langmuir* **2004**, *20*, 8970.
(13) Shashkina, J. A.; Philippova, O. E.; Zaroslov, Y. D.; Khokhlov, A. R.; Pryakhina, T. A.; Blagodatskikh, I. V. *Langmuir* **2005**, *21*, 1524.
(14) Croce, V.; Cosgrove, T.; Dreiss, C. A.; King, S.; Maitland, G.; Hughes, T. *Langmuir* **2005**, *21*, 6762.
(15) Warr, G. G.; Zemb, T. N.; Drifford, M. *J. Phys. Chem.* **1990**, *94*, 3086.
(16) Kalur, G. C.; Raghavan, S. R. *J. Phys. Chem. B* **2005**, *109*, 8599.

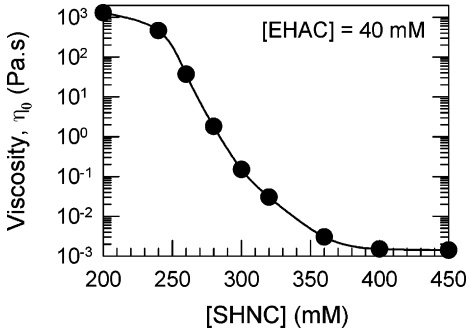

Figure 2. Zero-shear viscosity η_0 of EHAC/SHNC solutions at 25 °C as a function of SHNC concentration. The EHAC concentration is 40 mM.

points are observed only for c_{SHNC} between ca. 70 and 180 mM; at higher c_{SHNC}, the samples remain one-phase over the range of temperatures studied.

Rheology. Figure 2 shows the zero-shear viscosity η_0 at 25 °C of 40 mM EHAC solutions as a function of c_{SHNC}. Our focus is on the higher SHNC concentrations where the samples are one-phase at all temperatures—thus, the starting point on the abscissa of Figure 2 is 200 mM SHNC. Figure 2 shows that, as c_{SHNC} is increased from 200 to 450 mM, η_0 decreases monotonically by about 6 orders of magnitude. Thus, while the 450 mM sample has a viscosity similar to that of water, the 200 mM sample is highly viscoelastic and exhibits a very long relaxation time. In fact, some samples in the range 80−200 mM SHNC are almost gel-like in their behavior. A full discussion of EHAC/SHNC rheology over the entire range of salt concentrations will be reported in a separate publication.

We now describe the rheology of typical EHAC/SHNC samples as a function of temperature. In Figure 3, data are presented for the zero-shear viscosity η_0 as a function of temperature for three samples with $c_{EHAC} = 40$ mM and $c_{SHNC} = 240$, 260, and 280 mM, respectively. For the 240 mM sample, η_0 drops monotonically over the entire range of temperatures (Figure 3a). This is the expected trend in viscosity vs temperature for wormlike micellar fluids,[4] and similar behavior is seen for all samples below 260 mM salt. On the other hand, the 260 and 280 mM samples show a qualitatively different behavior. For the 260 mM sample (Figure 3b), η_0 increases from 25 °C up to around 35 °C and decreases at higher temperatures. Last, for the 280 mM sample (Figure 3c), η_0 increases in the temperature range between 25 to around 45 °C and then decreases at higher temperatures. The increase in η_0 in Figure 3c is fairly substantial—from ca. 2 Pa·s at 25 °C to its peak value ca. 15 Pa·s around 45 °C (factor of about seven increase).

Figure 3 thus reveals an unusual *increase* in viscosity with temperature in some EHAC/SHNC samples. This viscosity increase is completely reversible, i.e., when a sample is cooled, it returns to its original viscosity. We will now focus on the 280 mM sample and describe in more detail its rheological properties over the range of temperatures. Dynamic rheological spectra for this sample at different temperatures are presented in Figure 4. The plots show the elastic modulus G' and the viscous modulus G'' as functions of frequency ω. We note that the sample exhibits the viscoelastic response expected of wormlike micelles, with elastic behavior at high ω or short time scales (G' dominating over G'') and viscous behavior at low ω or long time scales (G'' exceeding G'). The (longest) relaxation time t_R of the sample can be estimated as $1/\omega_c$, where ω_c is the frequency at which G' and G'' cross over. Figure 4a shows data at 25 and 45 °C, and we note that the relaxation time t_R from the crossover point increases from ca. 0.3 s at 25 °C to ca. 2.5 s at 45 °C. Data at 50 and

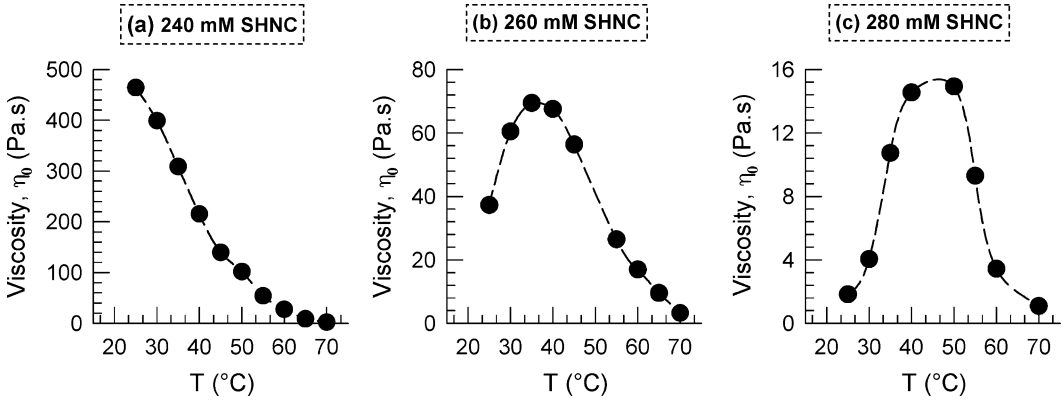

Figure 3. Zero-shear viscosity η_0 as a function of temperature for three different EHAC/SHNC solutions. The solutions each contain 40 mM EHAC.

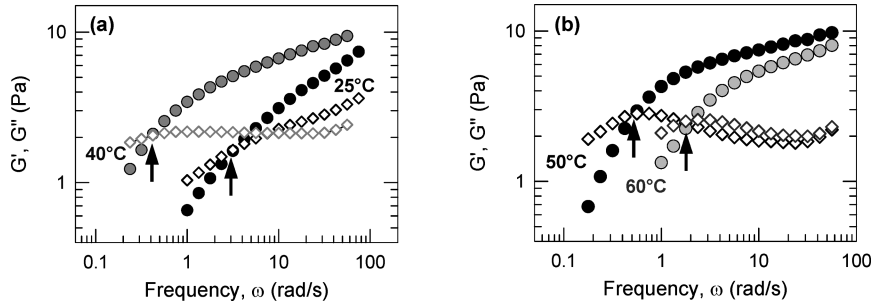

Figure 4. Dynamic rheology of a 40 mM EHAC + 280 mM SHNC sample at various temperatures. Data are shown for the elastic modulus G' (filled circles) and the viscous modulus G'' (unfilled diamonds) as functions of frequency. For clarity, the data are split into two plots: (a) 25 and 40 °C and (b) 50 and 60 °C. The arrows indicate the frequency at which G' and G'' intersect—the inverse of this frequency corresponds to the longest relaxation time of the sample.

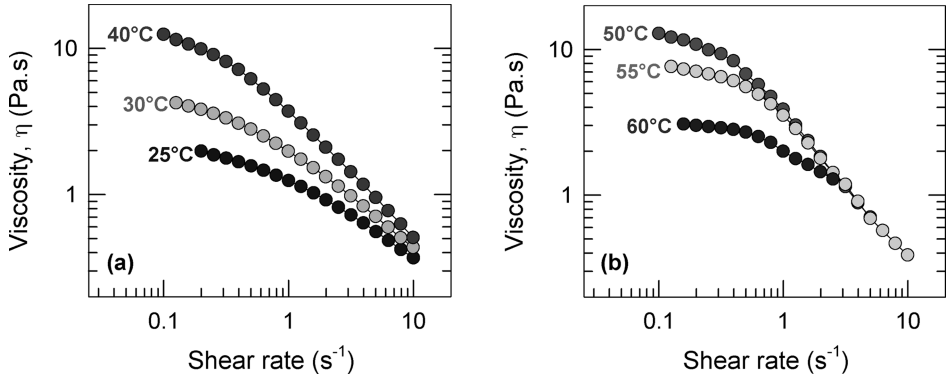

Figure 5. Steady-shear rheology (viscosity as a function of shear rate) for a 40 mM EHAC + 280 mM SHNC sample at various temperatures. For clarity, the data are split into two plots: (a) 25−40 °C and (b) 50−60 °C.

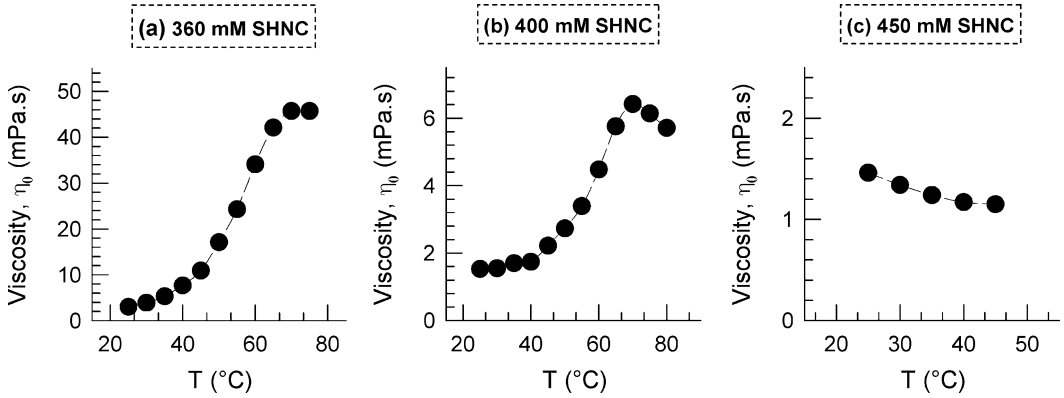

Figure 6. Zero-shear viscosity η_0 as a function of temperature for three different EHAC/SHNC solutions. The solutions each contain 40 mM EHAC.

60 °C are plotted in Figure 4b, and we observe here that the relaxation time drops from ca. 2 s at 50 °C to ca. 0.5 s at 60 °C. Dynamic rheology thus reveals an increase in relaxation time up to 45 °C and a subsequent decrease at higher temperatures.

Figure 5 shows the corresponding steady-shear rheological data at various temperatures for the 280 mM SHNC sample. In all cases, the viscosity exhibits a Newtonian plateau at low shear rates followed by shear-thinning at high shear rates. The zero-shear viscosity η_0 increases in the range from 25 to 45 °C (Figure 5a), whereas η_0 decreases beyond 50 °C (Figure 5b). The increase in low-shear viscosity mirrors the increase in relaxation time observed in Figure 4. The viscosity at high shear rates, on the other hand, is much less sensitive to temperature, a feature that has been seen in other studies on wormlike micellar solutions.[4]

We now return to examining the temperature dependence of EHAC/SHNC sample rheology for other SHNC concentrations. As c_{SHNC} is increased beyond 280 mM, the viscosity increase occurs over a wider range of temperatures. The sample starts at a lower viscosity, but the ratio of peak viscosity to initial viscosity is greater. This is shown by the data in Figure 6, where the zero-shear viscosity η_0 as a function of temperature is reported for three more samples with c_{SHNC} = 360, 400, and 450 mM, respectively. Note that the *y* axis for these data is in mPa·s, reflecting the lower viscosities of these samples compared to those in Figure 3. The sample with 360 mM SHNC exhibits a viscosity increase over the entire range of temperatures studied (Figure 6a). η_0 for this sample increases from ca. 2 to 50 mPa·s, which is a factor of 25 increase. The 400 mM sample shows an increase in η_0 from ca. 1.5 to 6 mPa·s at 70 °C (factor of 4 increase), followed by a decrease in η_0 at higher temperatures (Figure 6b). Finally, the 450 mM sample has a very low viscosity at room temperature (ca. 1.5 mPa·s) and there is a slight *decrease* in this viscosity upon heating (Figure 6c). Thus, a viscosity increase is only observed over a finite range of SHNC concentrations—for an EHAC concentration of 40 mM, it occurs between ca. 260 and 420 mM SHNC.

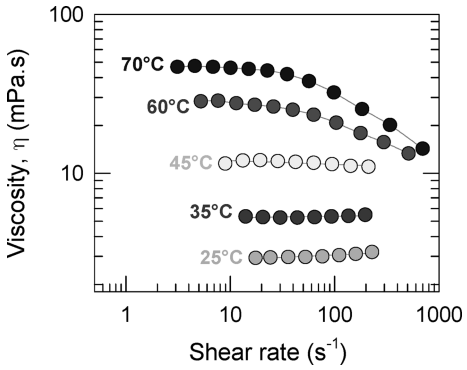

Figure 7. Steady-shear rheology (viscosity vs shear rate) for a 40 mM EHAC + 360 mM SHNC sample at various temperatures.

We now revisit the 360 mM sample and probe its rheology in some more detail. The steady-shear rheology of this sample over a range of temperatures is presented in Figure 7. At room temperature (25 °C), this sample is a Newtonian fluid with a viscosity of ca. 2 mPa·s (i.e., approximately twice that of water). Upon heating, the viscosity increases, while the sample continues to remain a Newtonian fluid. Around 60 °C, however, the rheology becomes non-Newtonian, with a shear-thinning response at high shear rates. The zero-shear viscosity continues to increase with temperature, and a similar response is seen at 70 °C as well (η_0 at 70 °C is ca. 50 mPa·s). The sample

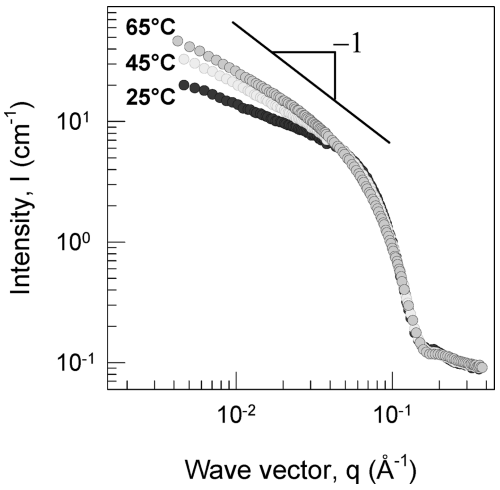

Figure 8. SANS scattering from a 40 mM EHAC + 360 mM SHNC sample at various temperatures.

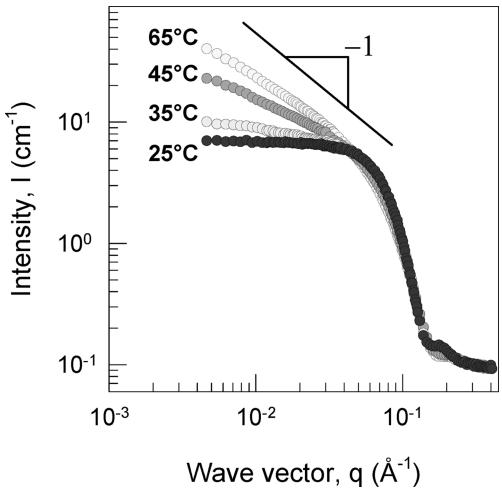

Figure 9. SANS scattering from a 40 mM EHAC + 400 mM SHNC sample at various temperatures.

thus changes from a Newtonian fluid at low temperatures to a viscous, non-Newtonian fluid at high temperatures. This is in direct contrast to the behavior of typical rodlike or wormlike micellar fluids, which usually transform from a highly viscous and non-Newtonian fluid at low temperatures to a Newtonian, low-viscosity fluid at high temperatures.

SANS. To understand the microstructural origins of the observed rheological changes, we turned to SANS. For these experiments, samples were made using D_2O instead of H_2O. We verified that the rheology of EHAC/SHNC samples in D_2O matched closely to that of the corresponding compositions in H_2O. Figure 8 shows SANS spectra (I vs q) at various temperatures from a sample containing 40 mM EHAC and 360 mM SHNC. Recall from Figure 6 that the viscosity of this sample monotonically increased with temperature. In turn, the SANS spectra show a monotonic rise in low-q intensity for this sample as the temperature is increased from 25 to 65 °C. The intensity at high q, on the other hand, remains practically unchanged with temperature. Note that these SANS spectra resemble those from long cylindrical micelles over the entire range of temperatures (e.g., the data asymptote to a slope close to −1 at low q).[17] The rise in low-q intensity thus signifies the growth of the cylindrical (wormlike) micelles, i.e., an *increase* in the micellar contour length, with increasing temperature. The constancy of the high-q data suggests that the micellar radius remains practically unchanged with temperature. The value of this radius can be obtained from a cross-sectional Guinier plot, i.e., a plot of $\ln(Iq)$ versus q^2 (not shown) and is found to be ca. 26 Å. For comparison, the length of a fully extended 22-carbon saturated alkyl tail is estimated to be ca. 29 Å from the Tanford formula.[18]

Similar upturns in low-q intensity are seen for other EHAC/SHNC samples that exhibit a viscosity increase with temperature. Of particular interest is a sample containing 40 mM EHAC + 400 mM SHNC, data for which are shown in Figure 9. Rheological measurements for this composition in H_2O (Figure 6) showed a monotonic rise in viscosity between 25 and 65 °C, but the low viscosities (1.5−6 mPa·s) suggested that the micelles present must be rather small (and thereby more amenable to analysis within the length scales probed by SANS). Indeed, the SANS data in Figure 9 show significant changes between 25 and 65 °C. At low temperatures (25 and 35 °C), there is a plateau in the low-q intensity, and the scattering curve is suggestive of small spherical or ellipsoidal micelles. With increasing temperature, there is a dramatic increase in the low-q intensity and the spectra begin to resemble that of cylindrical or long ellipsoidal micelles. Thus, a systematic growth of micelles with increasing temperature is qualitatively evident from the SANS data.

For a more quantitative analysis of the data in Figure 9, we use the indirect Fourier transform (IFT) method, which enables analysis of SANS data without assuming any a priori knowledge about the scatterers.[19] In this analysis, a Fourier transformation of the scattering intensity $I(q)$ yields the pair distance distribution function $p(r)$ in real space. The two are related by the following equation:[19]

$$I(q) = 4\pi \int_0^\infty p(r) \frac{\sin(qr)}{qr} \, dr \qquad (1)$$

The $p(r)$ function provides structural information about the scatterers in the sample. In particular, the maximum dimension of the scattering entities can be estimated. Note that, in the simplest form of the IFT technique, it is assumed that the scatterers do not interact.[19] Before implementing the IFT methodology, it is useful to first subtract the incoherent background from the scattering data. This background was estimated from the asymptotic slope of a Porod plot ($I(q)q^4$ vs q^4). The IFT calculation was then performed on the reduced data using the commercially available PCG software package.

Figure 10 shows the resulting $p(r)$ functions for each of the scattering curves in Figure 9 without considering any interparticle interactions. At 25 and 35 °C, the $p(r)$ functions are symmetrical, which here is indicative of spherical micelles. The maximum in $p(r)$, which is akin to a "most probable distance between adjacent scatterers", corresponds to the radius of the spheres, and $p(r) \rightarrow 0$ at a value of r corresponding to the micellar diameter, i.e., twice the radius.[19] The value of this micellar diameter is around 60 Å at 25 °C and 70 Å at 30 °C. At 45 °C, the $p(r)$ becomes asymmetrical and exhibits a shallow second peak. In this case, $p(r) \rightarrow 0$ at a much larger value of r (~400 Å), which gives an upper limit on the size of the structures

(17) *Neutron, X-Ray and Light Scattering: Introduction to an Investigative Tool for Colloidal and Polymeric Systems*; Zemb, T.; Lindner, P., Eds.; Elsevier: Amsterdam, 1991.

(18) Tanford, C. *The Hydrophobic Effect*, 2nd ed.; Wiley: New York, 1980.

(19) Glatter, O. *J. Appl. Crystallogr.* **1977**, *10*, 415.

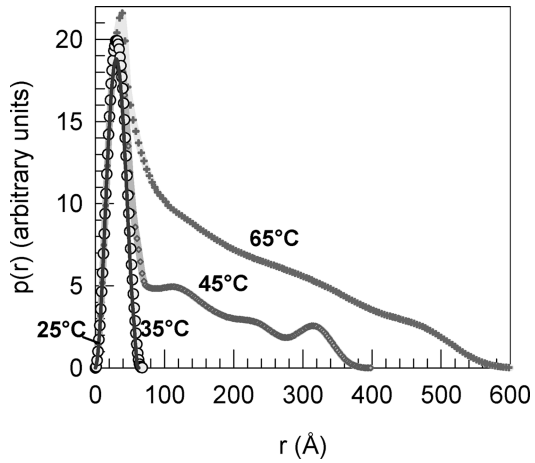

Figure 10. Pair distance distribution functions $p(r)$ corresponding to the SANS data in Figure 9 obtained at various temperatures for a 40 mM EHAC + 400 mM SHNC sample. The $p(r)$ curves were obtained by an indirect Fourier transformation (IFT) of the data without considering any interparticle interactions (see text for details).

present. A shoulder or second peak in $p(r)$ is often indicative of interactions between the scatterers, which complicates the interpretation of $p(r)$.[20−22] Nevertheless, it is clear that the structures at 45 °C are larger than at the lower temperatures. Finally, at 65 °C, the $p(r)$ becomes strongly asymmetrical and exhibits an inflection point followed by an approximately linear decrease. Such a linear decrease is characteristic of cylindrical micelles.[20,21] In this case, the $p(r)$ tends to zero around 600 Å, which provides an estimate for the maximum length of the cylinders. Our analysis of the SANS data by the IFT method thus reveals a growth of micelles from compact spheres at 25 °C to elongated cylinders at 65 °C.

4. Discussion

We have demonstrated an increase in viscosity with temperature in solutions of 40 mM EHAC over a range of SHNC concentrations (260−420 mM). Using rheology and SANS, we have shown that the increase in viscosity is due to the growth of cylindrical micelles with increasing temperature. The viscosity increase is quite substantial—more than an order of magnitude for many samples. It is worth reiterating that such an increase in viscosity is very unusual in the case of cationic wormlike micellar solutions. Specifically, in the case of micelles formed by the EHAC cationic surfactant, a viscosity increase has not been previously reported to our knowledge. Note that EHAC has been studied in conjunction with a range of salts, including simple salts such as NaCl and KCl, as well as binding counterions such as NaSal and sodium tosylate.[4,9] None of these samples, however, showed an increase in viscosity with temperature.

The question then is why we see the viscosity increase with SHNC and not with other salts. In particular, why does SHNC behave differently compared to NaSal, despite the two counterions being closely related (Figure 1)? A further intriguing question is, why do we see the viscosity increase only over a limited range of SHNC concentrations? These questions are related, and we will try to tackle them together. The significant difference between SHNC and NaSal is that the hydrophobic moiety is bulkier in SHNC. In turn, this causes SHNC to have a lower solubility in water compared to NaSal.[23] Thus, when added to water in the presence of cationic micelles, the HNC^- counterions will partition almost entirely to the micelles, with their aromatic portion submerged within the hydrophobic interior of the micelles (see Figure 11). Even when there is an excess of HNC^- over surfactant molecules, the strongly hydrophobic nature of the counterions will induce the vast majority of them to segregate toward the micelles. (For simplicity, we assume that the counterions tend to become uniformly distributed over the entire micelle. Although naphthalene derivatives can π-stack, it is not clear if this will impact the distribution of HNC^- at the micellar interface.).

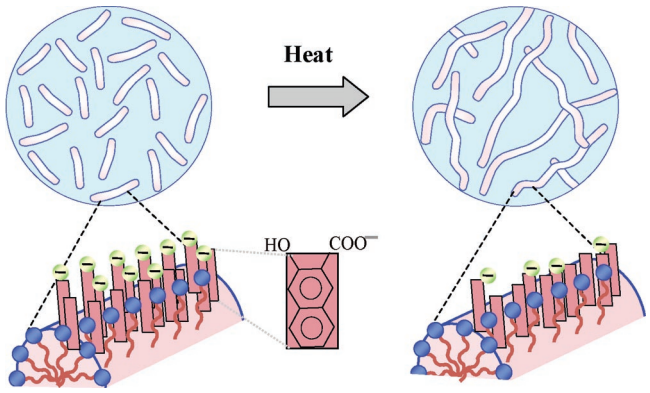

Figure 11. Schematic of the micellar structure in a 40 mM EHAC + 360 mM SHNC solution at low and high temperatures. At low temperatures (left), the micelles are depicted to be short cylinders or ellipsoids. In this case, most of the HNC^- counterions are shown bound to the micelle, due to which the micelle bears a strong negative charge. At high temperatures (right), the micelles have grown into longer, flexible cylinders (wormlike micelles). This growth is attributed to the desorption of some of the bound HNC^- counterions and the consequent reduction in micellar surface charge.

To illustrate the consequences of counterion binding, take the specific example of a particular EHAC/SHNC composition, say 40 mM EHAC + 360 mM SHNC. In this case, there are nine times as many SHNC molecules as EHAC, and all of the HNC^- counterions are likely to be bound to the micelles. Because of the large excess of counterions, not all these ions may be bound strongly, i.e., some HNC^- ions may only be partially inserted into the micelles. This is the scenario we expect at low temperatures, and it is depicted schematically on the left-hand side of Figure 11. Note that, because of the large fraction of bound anions, the micellar interface is expected to bear a strong negative charge. Due to this unscreened charge, the micelles existing in solution are likely to be highly curved structures, i.e., mostly spherical or slightly elongated micelles. Now consider what happens upon increasing temperature. The solubility of SHNC in water is expected to increase with temperature, which means a reduction in the tendency of HNC^- counterions to bind onto the micelles.[23] This may cause some of the weakly bound counterions to desorb from the micelles and release into solution (the resulting micellar interface is depicted schematically on the right-hand side of Figure 11). In turn, we suggest that the micellar surface charge is reduced, thereby leading to a growth of cylindrical micelles with increasing temperature.

The above mechanism is the simplest one that can account for our results. It can be used to explain why the

(20) Glatter, O.; Fritz, G.; Lindner, H.; Brunner-Popela, J.; Mittelbach, R.; Strey, R.; Egelhaaf, S. U. *Langmuir* **2000**, *16*, 8692.
(21) Raghavan, S. R.; Fritz, G.; Kaler, E. W. *Langmuir* **2002**, *18*, 3797.
(22) Hassan, P. A.; Fritz, G.; Kaler, E. W. *J. Colloid Interface Sci.* **2003**, *257*, 154.
(23) Hassan, P. A.; Valaulikar, B. S.; Manohar, C.; Kern, F.; Bourdieu, L.; Candau, S. J. *Langmuir* **1996**, *12*, 4350.

viscosity increase occurs only over a certain range of SHNC concentrations. The key point is that, if the micelles are already very long at room temperature, any desorption of counterions will have a negligible effect on the micelle curvature. It should be noted that temperature exerts a competing effect, which is to exponentially decrease the micelle contour length (this is ultimately the reason the viscosity goes through a maximum for many samples). Thus, it is only for micelles that are *quite short to begin* with (*as indicated by a low viscosity at room temperature*) that we see the effects related to counterion desorption. This can explain why the viscosity increase only occurs for $c_{SHNC} > 260$ mM. On the other hand, the effect is masked for $c_{SHNC} > 450$ mM because in these cases the micelles are so swamped with HNC^- counterions that the desorption of a few ions has a negligible effect on micelle charge, and hence curvature.

A similar series of arguments was advanced by Manohar et al.[23−25] to describe a temperature-induced transition from multilamellar vesicles to wormlike micelles in solutions of the surfactant cetyl trimethylammonium hydroxynaphthoate (CTA-HNC). In this case, the HNC^- formed the counterions for the surfactant, and at low temperatures, these counterions remained bound to the surfactant. The resulting low surface charge lead to the formation of vesicular aggregates. However, at high temperatures, the authors postulated a desorption of some HNC^- counterions from the aggregates, resulting in an increased charge and thereby a transition from vesicles to wormlike micelles.[24,25] Note that, in the case of CTA-HNC, there was always an equimolar concentration of surfactant molecules and counterions, whereas in our samples, we have a large excess of HNC^- counterions over surfactant molecules. Therefore, the desorption of counterions has a different consequence in our case than in that studied by Manohar et al.

One final question is whether the viscosity increase in EHAC/SHNC samples is connected with the cloud-point phenomenon observed at lower SHNC compositions (Figure 1). To reiterate, the EHAC/SHNC solutions that show a viscosity increase *do not* show cloud points over the accessible range of temperatures. Also, the solutions that have cloud points do not show a viscosity increase—their viscosity decreases monotonically with temperature until their cloud point (much like for the 240 mM sample in Figure 3a). Similar trends in viscosity have been reported for EHAC/NaSal samples that had cloud points.[9] In this earlier study, the cloud point was attributed either to attractive interactions between micelles or to a transition from linear to branched micelles with increasing temperature.[9] Thus, the viscosity increase observed here appears to have a different origin compared to the cloud-point phenomenon.

Conclusions

In this paper, we have reported unusual rheological behavior in micellar solutions of the cationic surfactant EHAC and the binding salt, SHNC. Over a range of SHNC concentrations corresponding to a large excess of counterions over surfactant, these solutions show an increase in viscosity with temperature. The viscosity increase can be fairly substantial, often exceeding an order of magnitude. For some samples, the viscosity rises to a peak and thereafter decreases. Using SANS, we have shown that the increase in viscosity is caused by an increase in the contour length of cylindrical micelles. We attribute this micellar growth to a desorption of weakly bound HNC^- counterions from the micelle at elevated temperatures. Such a desorption is believed to reduce the charge density at the micellar interface and thereby promote the growth of cylindrical structures.

Acknowledgment. We would like to acknowledge NIST for facilitating the SANS experiments performed as part of this work. This work was partially funded by a grant from NSF-CTS.

LA052069W

(24) Menon, S. V. G.; Manohar, C.; Lequeux, F. *Chem. Phys. Lett.* **1996**, *263*, 727.
(25) Narayanan, J.; Mendes, E.; Manohar, C. *Int. J. Mod. Phys. B* **2002**, *16*, 375.